symmetry

MDPI

Article

Radiation Properties of the Accretion Disk around a Black Hole Surrounded by PFDM

Bakhtiyor Narzilloev [1,2,3,4] and Bobomurat Ahmedov [1,5,6,*]

1 Ulugh Beg Astronomical Institute, Astronomy Street 33, Tashkent 100052, Uzbekistan
2 Akfa University, Milliy Bog' Street 264, Tashkent 111221, Uzbekistan
3 Samarkand State University, University Avenue 15, Samarkand 140104, Uzbekistan
4 Bukhara State University, Mukhammad Ikbol Street 11, Bukhara 705018, Uzbekistan
5 National University of Uzbekistan, Tashkent 100174, Uzbekistan
6 Tashkent Institute of Irrigation and Agricultural Mechanization Engineers, Kori Niyoziy 39, Tashkent 100000, Uzbekistan
* Correspondence: ahmedov@astrin.uz

Abstract: The thermal radiation properties of the accretion disk around a non-rotating black hole with a perfect fluid dark matter (PFDM) environment are investigated. A non-rotating black hole surrounded by perfect fluid dark matter together with a classical geometrically thin but optically thick Novikov–Thorne disk is selected as a system to be analyzed. It is observed that the perfect fluid dark matter strengthens the gravitational field, which leads to both the increase of the radii of the event horizon and the innermost stable circular orbit (ISCO). However, for the flux of the radiant energy over the accretion disk, the maximum flux is reduced and shifted outwards the central object under the influence of the perfect fluid dark matter. The dependence of the thermal profile of the disk on the radial coordinate and the intensity of perfect fluid dark matter shows analogous behavior. It has been demonstrated that the radiative efficiency of the accretion disk is increased from ∼6% up to ∼20% with the increase in the intensity of the surrounding perfect fluid dark matter. The thermal spectra of the accretion disk has also been explored, which is shifted towards the lower frequencies (corresponding to the gravitational redshift of the electromagnetic radiation coming from the disk) with the increase in the intensity of the perfect fluid dark matter.

Keywords: black hole; dark matter; accretion disk; general relativity

Citation: Narzilloev, B.; Ahmedov, B. Radiation Properties of the Accretion Disk around a Black Hole Surrounded by PFDM. *Symmetry* **2022**, *14*, 1765. https://doi.org/10.3390/sym14091765

Academic Editors: Kazuharu Bamba and Axel Pelster

Received: 20 July 2022
Accepted: 22 August 2022
Published: 24 August 2022

1. Introduction

Einstein's general relativity (GR) is consistent with very good precision with observations only in the weak field approximation in the Solar system. On other hand, cosmological and astronomical observation of new forms of matter, such as dark matter in galactic and intergalactic large cosmic web scale and dark energy in the cosmological scale in our universe [1], provides strong evidence to include an energy momentum tensor representing an exotic hypothetical form of dark energy called quintessence and dark matter into the right hand side of Einstein's field equations for fitting the currently available data, which leads to the modified BH solutions [2–8]. Kiselev, in a pioneering study [2,8], developed new models for dark matter to be treated as a perfect fluid, and later, a new black hole solution surrounded by PFDM was explored in [9]. Various optical, radiative and energetic properties of several astrophysical black holes were investigated in our preceding studies (see, e.g., [10–14]).

From an astrophysical point of view, comparison of observational data on thin accretion to astrophysical black holes with inclusion of the expected thermal spectra can provide a powerful tool to test the strong-field regime of gravity. Motivated by this opportunity, we investigate in this work the properties of innermost stable circular orbits in spacetime of non-rotating black hole surrounded by PFDM and analyze the main features of the

geometrically thin Novikov–Thorne model for the accretion disk around the black hole, which is treated as an optically thick disk. In particular, we present temperature and spectral energy distributions for a thin Novikov–Thorne disk and compare the obtained results with those obtained using the standard black holes in the framework of GR.

The paper is constructed in the following way: in Section 2, the properties of the spacetime around non-rotating BH with PFDM environment are discussed. In Section 3, we present the Novikov–Thorne model for an accretion disk of a central BH surrounded by PFDM, which is geometrically thin but optically thick. The flux of the radiant energy over the accretion disk, radiative efficiency of the disk, temperature profile, and the spectrum of the radiation emitted from the surface of the disk due to the thermal radiation are discussed in Section 4. Section 5 summarizes the main results obtained in the paper. The geometrized units $G = c = 1$ are used, Greek indices are selected to run $0, 1, 2, 3$, and the signature of the spacetime is taken as timelike $(-,+,+,+)$.

2. Spacetime of Black Hole Surrounded by PFDM

The spacetime metric of non-rotating BH with mass M surrounded by PFDM has the following form [15]:

$$\begin{array}{rcl} ds^2 & = & -f(r)dt^2 + f(r)^{-1}dr^2 + r^2 d\Omega^2, \\ f(r) & = & 1 - \frac{2M}{r} - \frac{\alpha}{r}\log\frac{r}{|\alpha|}\,. \end{array} \tag{1}$$

Here, the parameter α takes into account the density and pressure of PFDM. The known Schwarzschild spacetime is recovered in the limiting case when the extra spacetime parameter α tends to zero.

The energy-momentum tensor of the PFDM

$$T^{\mu}_{\nu} = \mathrm{diag}(-\rho, p_r, p_\theta, p_\phi)\,, \tag{2}$$

is given through the relationship between the pressure and the density of the PFDM as

$$\rho = -p_r = -\frac{\alpha}{8\pi r^3} \quad \text{and} \quad p_\theta = p_\phi = -\frac{\alpha}{16\pi r^3}\,. \tag{3}$$

assuming that the parameter $\alpha > 0$.

The behavior of the lapse function with the change of the radial coordinate is given in Figure 1 for the different values of the parameter α. It is clearly seen from the figure that the function tends to 1 as the radial coordinate tends to infinity, which, in turn, reduces the given spacetime metric to the Minkowski spacetime written in Boyer–Lindquist coordinates. One can also see that in the close environment of the central compact gravitating object, an increase in the intensity of PFDM impacts the spacetime geometry. This impact should have an effect on the electromagnetic radiation and other properties of the accretion disk around a black hole in the center. The main aim of this work is to investigate such effects.

One can find the location of the event horizon radius as the function of the intensity of PFDM from the condition $f(r) = 0$ as presented in Figure 2 with a black solid line. We see that increasing α makes the event horizon become bigger, making the gravitational field stronger. Indeed, when the gravitational field becomes stronger, a black hole can capture particles (photons) emitted at farther distances, making the size of the event horizon bigger.

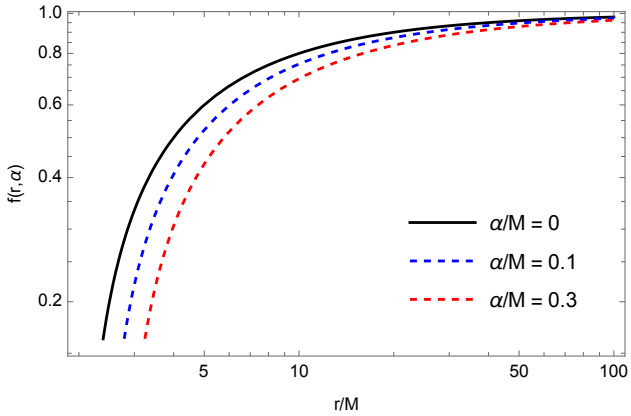

Figure 1. Radial dependence of the lapse function for the selected values of the intensity parameter of PFDM.

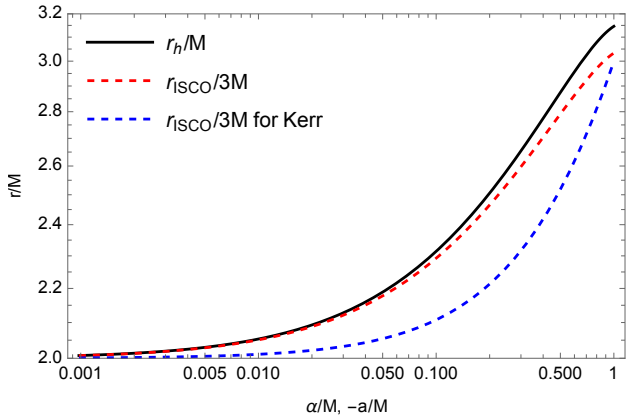

Figure 2. Dependence of the event horizon radius (black solid line) and the ISCO radius (red dashed line) on the intensity parameter of perfect fluid dark matter around a central black hole in comparison with the dependence of the ISCO radius from the spin parameter in the Kerr spacetime (blue dashed line).

3. Novikov–Thorne Model of the Accretion Disk

We assume that the accretion disk formed around the central BH surrounded by PFDM is geometrically thin but optically thick according to the Novikov–Thorne model used [16]. In terms of vertical size, the thin accretion disk is always negligible, as compared to its comparatively long horizontal extension. Accordingly, the accretion disk height h, being equal to the maximum half thickness of the disk in the vertical direction, is always much smaller than the characteristic radius r of the disk in the horizontal direction; that is, $h \ll r$. The pressure gradient and a vertical entropy gradient in the accreting matter are negligible according to hydrodynamic equilibrium in the thin disk. The disk is prevented from accumulation of the heat generated by stresses and dynamical friction due to the efficient cooling through the thermal radiation over the whole disk surface. Consequently, the thin vertical size of the disk is stabilized by this equilibrium. An inner edge of the thin disk is at the marginally stable orbit around the compact object, and the accreting plasma takes a classical Keplerian motion in the higher orbits.

The mass accretion rate $\dot{M}_0$ does not depend on time in steady-state accretion disk models. The orbiting plasma is described by the physical quantities averaged over a characteristic time scale, e.g., Δt, for a total period of the orbits over the azimuthal angle

$\Delta\phi = 2\pi$ and over the vertical height h [16–18]. The effective potential of particle with mass m moving in the equatorial plane of the central BH can be written as [16,18,19]

$$V_{\rm eff}(r) = -1 + \frac{E^2 g_{\phi\phi} + 2EL g_{t\phi} + L^2 g_{tt}}{g_{t\phi}^2 - g_{tt} g_{\phi\phi}}\,, \tag{4}$$

where the constants of motion E and L are a specific energy and a specific angular momentum of a test particle, respectively. These two conserved quantities can be expressed through the components of metric tensor as

$$E = -\frac{g_{tt} + \Omega g_{t\phi}}{\sqrt{-g_{tt} - 2\Omega g_{t\phi} - \Omega^2 g_{\phi\phi}}}\,, \tag{5}$$

and

$$L = \frac{\Omega g_{\phi\phi} + g_{t\phi}}{\sqrt{-g_{tt} - 2\Omega g_{t\phi} - \Omega^2 g_{\phi\phi}}}\,. \tag{6}$$

Here, the angular velocity is

$$\Omega = \frac{d\phi}{dt} = \frac{-g_{t\phi,r} \pm \sqrt{\{-g_{t\phi,r}\}^2 - \{g_{\phi\phi,r}\}\{g_{tt,r}\}}}{g_{\phi\phi,r}}\,. \tag{7}$$

In the chosen model, the inner edge of the accretion disk around the central black hole coincides with the ISCO of test particles orbiting the massive gravitating object in the center. From the following set of conditions on the effective potential of the test particle

$$V_{\rm eff}(r) = 0\,, \quad V'_{\rm eff}(r) = 0\,, \quad V''_{\rm eff}(r) = 0\,, \tag{8}$$

one can find the location of ISCO as the function of the extra spacetime parameter, as demonstrated in Figure 2 with the red dashed line. It is apparent from the figure that increase in the intensity of PFDM makes the ISCO radius bigger, as in the case of the event horizon radius, due to the same reason explained before. One can also see from the figure that, for the retrograde motion of particles around a Kerr black hole, a similar increase in the values of the ISCO radius can be obtained (blue dashed line). This similarity motivated us to plot the degeneracy between the spin parameter and the intensity of PFDM for matching values of the ISCO radii, as presented in Figure 3. It is clearly demonstrated in the figure that the intensity of PFDM indeed can mimic the effect of spin on the ISCO radius for the retrograde motion of particles in the inner edge of the accretion disk. The value of α/M to completely mimic the retrograde spin appears to be around $\sim$0.88, as seen from the figure.

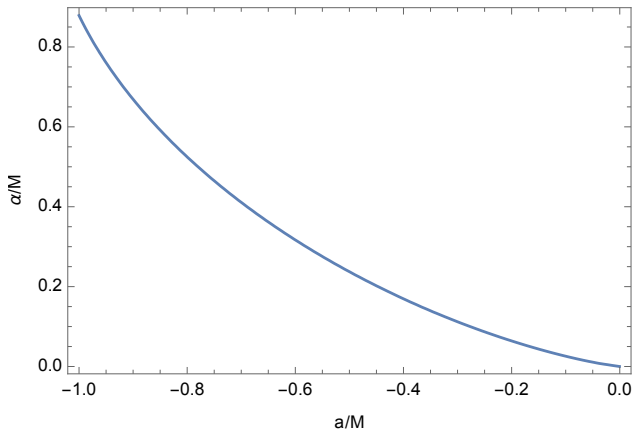

Figure 3. The degeneracy between PFDM parameter α and BH spin parameter a through the ISCO location.

4. Radiative Properties of the Accretion Disk around a Central Compact Object

As for the properties of the accretion disk, we will mainly focus on the flux of the radiant energy over the disk, radiative efficiency of the disk, temperature profile, and the spectrum of the radiation emitted from the disk due to the thermal radiation.

The flux of the electromagnetic radiation emitted from the accretion disk is given by the following expression: [16,18]

$$F(r) = -\frac{\dot{M}_0 c^2}{4\pi M^2} \frac{\Omega_{,r}}{\sqrt{-g}(E-\Omega L)^2} \int_{r_{ISCO}}^{r} (E-\Omega L) L_{,r} dr, \tag{9}$$

where g is the determinant of the metric tensor. The radial dependence of the flux of the radiant energy over the disk for the various values of the intensity of PFDM is shown in Figure 4. We see that the maximum flux in the case of the Schwarzschild spacetime (when $\alpha = 0$) is always greater than the case when PFDM comes to the game. It is clearly seen that an increase in the intensity parameter of PFDM not only reduces the maximum value of the flux but also shifts this maximum towards a greater radial coordinate. It is also noticeable that the points where the flux becomes zero also shift towards greater r. These points give us the closest part of the disk, which is visible due to the radiation emitted by particles in that regions. Such regions defines the inner edge of the accretion disk, which, in turn, coincides with innermost stable circular orbits of test particles, and we have seen that an increase in α indeed makes such orbits bigger (see Figure 2).

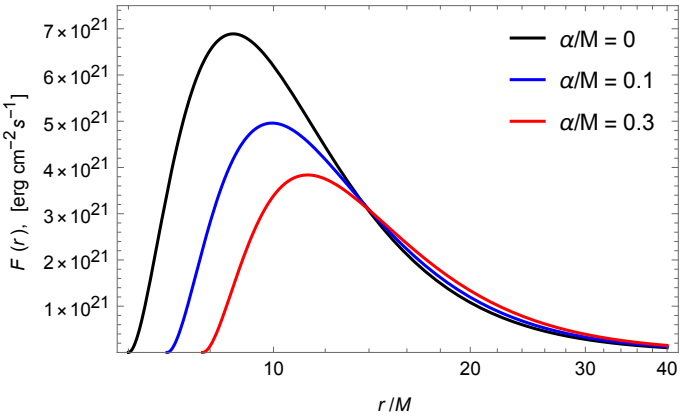

Figure 4. Radial profile of the flux of electromagnetic radiation of the disk for the different values of the PFDM parameter α.

The efficiency with which the central object converts rest mass-accreting matter into outgoing electromagnetic radiation is the most important property of the mass accretion process. The ratio of two quantities measured at infinity [16,18] as the radiation rate of energy of photons emitted from the surface of disk and escaped to infinity to the rate at which mass energy is transported to the central BH determines the efficiency. If all the emitted photons can escape to infinity, the efficiency can be expressed through the specific energy measured at the ISCO as

$$\eta = 1 - E_{\mathrm{ISCO}} \,. \tag{10}$$

From this relation and expression for the specific energy (5), one can get the values of η in a table form, as shown in Table 1. One can see that the radiative efficiency increases with an increase in the intensity of PFDM.

Table 1. Change in the ISCO radius and the radiative efficiency of the accretion disk with the change in the intensity parameter of PFDM.

α/M	$r_{\rm ISCO}/M$	$\eta\%$
0.1	6.878	6.397
0.2	7.396	6.970
0.3	7.792	7.487
0.4	8.111	7.969
0.5	8.374	8.427

From the numerical calculus, one can also obtain the dependence between the radiative efficiency of the disk and the spacetime parameter α in a plot form, as demonstrated in Figure 5. It is shown that, being around 6% for the Schwarzschild spacetime, the line then goes up with the rise of the parameter α up to around 20%. Thus, one can conclude that the presence of the dark matter around a black hole increases the radiative efficiency of the disk monotonically.

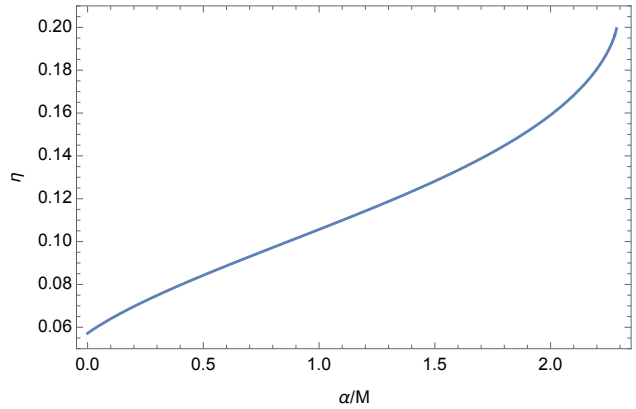

Figure 5. Monotonic growth of the efficiency of thermal radiation from disk with the increase in the PFDM parameter α.

Since the flux of the black body radiation can be written as $F = \sigma T^4$, where σ is the Boltzmann constant, one can show the radial profile of the disk temperature as demonstrated in Figure 6. One can see the similar behavior of the lines with the change in the intensity parameter of perfect fluid dark matter surrounding the central compact object, as in the case of the flux. In the left and right panels of Figure 6, the thermal profile of the disk in the units of Kelvin and in the units of energy are given a place, respectively.

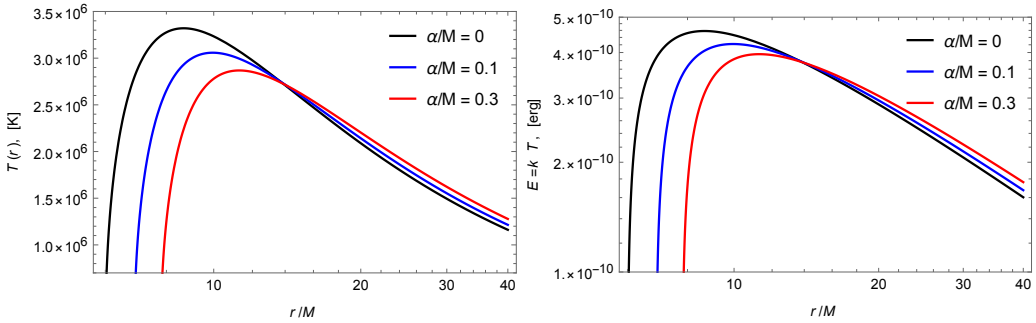

Figure 6. Temperature profile of the disk for the different values of the spacetime parameter α. On the left, the temperature is given in the units of Kelvin (K), and on the right, in the units of energy (erg).

One can be more informative to demonstrate the dependence of the temperature profile from the radial coordinate and the extra spacetime parameter in a "density-plot" form, as shown in the left panel of Figure 7. One can now clearly see the dark region inside

the inner edge of the accretion disk, which increases in size with the rise of α and once more demonstrates the change of the ISCO location with the change in α. The red parts represent the regions close to the maximum temperature of the disk that shift towards large distances when α goes up. The disk then cools down with the increase in the radial coordinate, as shown in the picture with green regions. The last one is even more demonstratively shown in the right panel of Figure 7 for the fixed $\alpha = 0.3$. The black round in the center represents the black hole with the same event horizon radius as the radius of this round. One can see that the temperature starts increasing sharply from zero to a few millions of Kelvin (thin region between the red and dark regions), reaches its maximum (inner parts of the red region), and then starts cooling down smoothly with increasing distance from the central compact object (outer regions).

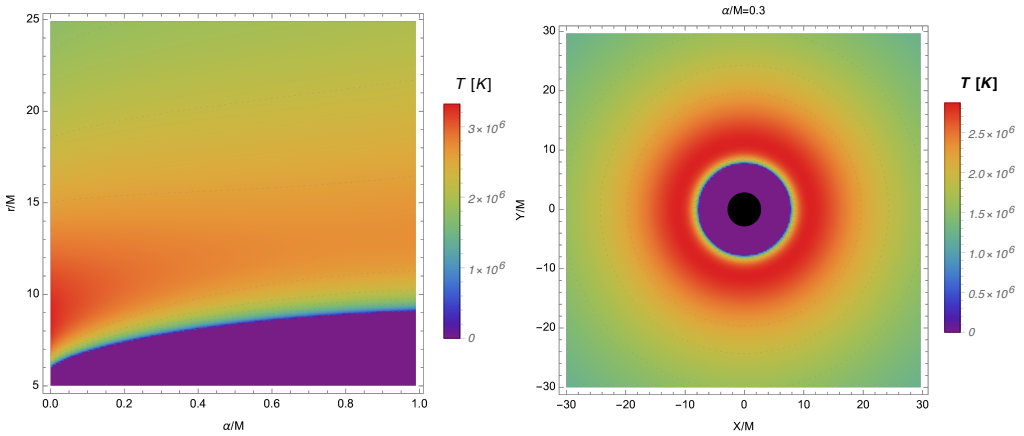

Figure 7. Temperature profile in the density-plot form. In the right panel, X and Y define the Cartesian coordinates, with the X-Y plane lying on the equatorial plane.

The luminosity of the radiation can be found from the following expression [20]:

$$L(\nu) = 4\pi d_L^2 I(\nu) = \frac{8}{\pi} \cos i \int_{r_{in}}^{r_{ex}} \int_0^{2\pi} \frac{\nu_e r d\phi dr}{\exp(\nu_e/T) - 1}, \tag{11}$$

where d_L denotes the distance from an observer to the far source, i denotes the inclination angle of the accretion disk, r_{in} is the inner edge and r_{ex} is the external edge of the disk, and $I(\nu)$ is the Planck distribution function. One can select $r_i = r_{\mathrm{ISCO}}$ and $r_o \to \infty$ due to the fact that at the asymptotic infinity, when $r \to \infty$, the flux over the disk surface vanishes as for any astronomical object. The emitted frequency $\nu_e = \nu(1+z)$ is given through the redshift factor z, which can be written in the form

$$1 + z = \frac{1 + \Omega r \sin\phi \sin i}{\sqrt{-g_{tt} - 2\Omega g_{t\phi} - \Omega^2 g_{\phi\phi}}}, \tag{12}$$

where the light bending is neglected [21,22]. The spectrum of the disk is presented in Figure 8 for the fixed values of the intensity parameter of PFDM. It is noticeable that an increase in the parameter α shifts the peak of the lines towards the lower frequencies. One can interpret this phenomena in the following way. Since the increase in the intensity of perfect fluid dark matter strengthens the gravitational field in total, the energy of escaping photons becomes smaller and reflects in the thermal spectrum of the disk. This is shown even more clearly in the right panel of the figure. It can be calculated that an increase in the PFDM intensity from 0 to 0.3 M can decrease the frequency of photons, corresponding to the peak of the spectra, by approximately 23%.

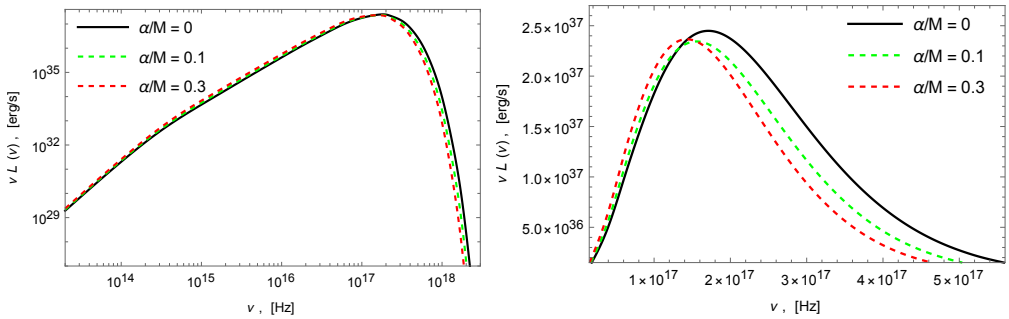

Figure 8. Spectra of the accretion disk around a non-rotating black hole surrounded by perfect fluid dark matter. The inclination angle is chosen to be $i = \pi/6$. Graph in the left is shown in the logarithmic scale, while the graph in the right is plotted in the ordinary scale in the close region to the maxima of the lines.

5. Summary

In this work, the effect of the perfect fluid dark matter on the properties of the accretion disk around a non-rotating black hole solution in GR has been investigated. The model considered was a system consisting of a Schwarzschild black hole surrounded by perfect fluid dark matter and a geometrically thin but optically thick Novikov–Thorne disk. It was shown through the behavior of the event horizon radius and the ISCO radius that, with an increase in the values of the intensity of the perfect fluid dark matter, the resultant gravitational field becomes stronger. Our study of the flux of the radiant energy over the disk has shown that an increase in the intensity of perfect fluid dark matter reduces the maximum flux and shifts it towards larger orbits. Similar behavior has been detected in the change in the thermal profile of the disk with the change in the radial coordinates and the intensity of the perfect fluid dark matter. We have also shown the change in the radiative efficiency of the accretion disk and demonstrated that the efficiency is increased from ∼6% up to ∼20% with the increase in the intensity of perfect fluid dark matter. Lastly, the spectra of the accretion disk has been studied. We demonstrated that an increase in the intensity of perfect fluid dark matter shifts the spectra towards lower frequencies, corresponding to the gravitational redshift of the electromagnetic radiation coming from the disk.

Author Contributions: Writing—original draft, B.N.; Writing—review and editing, B.A. All authors have read and agreed to the published version of the manuscript.

Funding: Ministry of Innovative Development of the Republic of Uzbekistan: Grants F-FA-2021-432 and MRB-2021-527.

Institutional Review Board Statement: Not applicable.

Informed Consent Statement: Not applicable.

Data Availability Statement: The data that support the findings of this study are available from the first author, Bakhtiyor Narzilloev, upon reasonable request.

Acknowledgments: This research is supported by Grants F-FA-2021-432 and MRB-2021-527 of the Uzbekistan Ministry for Innovative Development.

Conflicts of Interest: The authors declare no conflict of interest.

References

1. Planck Collaboration. Planck 2015 results. XIII. Cosmological parameters. *Astron. Astrophys.* **2016**, *594*, A13. [CrossRef]
2. Kiselev, V.V. Quintessence Black Holes. *Class. Quantum Gravity* **2003**, *20*, 1187–1197. [CrossRef]
3. Toshmatov, B.; Stuchlík, Z.; Ahmedov, B. Rotating black hole solutions with quintessential energy. *Eur. Phys. J. Plus* **2017**, *132*, 98. [CrossRef]
4. Abdujabbarov, A.; Toshmatov, B.; Stuchlík, Z.; Ahmedov, B. Shadow of the rotating black hole with quintessential energy in the presence of plasma. *Int. J. Mod. Phys.* **2017**, *26*, 1750051. [CrossRef]

5. Shaymatov, S.; Ahmedov, B.; Stuchlík, Z.; Abdujabbarov, A. Effect of an external magnetic field on particle acceleration by a rotating black hole surrounded with quintessential energy. *Int. J. Mod. Phys.* **2018**, *27*, 1850088. [CrossRef]
6. Chakrabarty, H.; Abdujabbarov, A.; Bambi, C. Scalar perturbations and quasi-normal modes of a nonlinear magnetic-charged black hole surrounded by quintessence. *Eur. Phys. J.* **2019**, *79*, 179. [CrossRef]
7. Benavides-Gallego, C.A.; Abdujabbarov, A.; Bambi, C. Rotating and nonlinear magnetic-charged black hole surrounded by quintessence. *Phys. Rev. D* **2020**, *101*, 044038. [CrossRef]
8. Kiselev, V.V. Quintessential solution of dark matter rotation curves and its simulation by extra dimensions. *arXiv* **2003**, arXiv:Gr-qc/0303031. Available online: https://arxiv.org/abs/gr-qc/0303031 (accessed on 7 April 2003).
9. Li, M.H.; Yang, K.C. Galactic dark matter in the phantom field. *Phys. Rev. D* **2012**, *86*, 123015. [CrossRef]
10. Narzilloev, B.; Malafarina, D.; Abdujabbarov, A.; Ahmedov, B.; Bambi, C. Particle motion around a static axially symmetric wormhole. *Phys. Rev. D* **2021**, *104*, 064016. [CrossRef]
11. Rayimbaev, J.; Narzilloev, B.; Abdujabbarov, A.; Ahmedov, B. Dynamics of Magnetized and Magnetically Charged Particles around Regular Nonminimal Magnetic Black Holes. *Galaxies* **2021**, *9*, 71. [CrossRef]
12. Narzilloev, B.; Rayimbaev, J.; Abdujabbarov, A.; Ahmedov, B. Regular Bardeen Black Holes in Anti-de Sitter Spacetime versus Kerr Black Holes through Particle Dynamics. *Galaxies* **2021**, *9*, 63. [CrossRef]
13. Narzilloev, B.; Hussain, I.; Abdujabbarov, A.; Ahmedov, B.; Bambi, C. Dynamics and fundamental frequencies of test particles orbiting Kerr–Newman–NUT–Kiselev black hole in Rastall gravity. *Eur. Phys. J. Plus* **2021**, *136*, 1032. [CrossRef]
14. Narzilloev, B.; Hussain, I.; Abdujabbarov, A.; Ahmedov, B. Optical properties of an axially symmetric black hole in the Rastall gravity. *Eur. Phys. J. Plus* **2022**, *137*, 645. [CrossRef]
15. Zhang, H.X.; Chen, Y.; Ma, T.C.; He, P.Z.; Deng, J.B. Bardeen black hole surrounded by perfect fluid dark matter. *Chin. Phys. C* **2021**, *45*, 055103. [CrossRef]
16. Novikov, I.D.; Thorne, K.S. Astrophysics and black holes. In Proceedings of the Les Houches Summer School of Theoretical Physics: Black Holes, 1973, Les Houches, France, 1 August 1972; pp. 343–550.
17. Shakura, N.I.; Sunyaev, R.A. Black holes in binary systems. Observational appearance. *Astron. Astrophys.* **1973**, *24*, 337–355.
18. Page, D.N.; Thorne, K.S. Disk-Accretion onto a Black Hole. Time-Averaged Structure of Accretion Disk. *Astrophys. J.* **1974**, *191*, 499–506. [CrossRef]
19. Banerjee, I.; Chakraborty, S.; SenGupta, S. Decoding signatures of extra dimensions and estimating spin of quasars from the continuum spectrum. *Phys. Rev. D* **2019**, *100*, 044045. [CrossRef]
20. Torres, D.F. Accretion disc onto a static non-baryonic compact object. *Nucl. Phys. B* **2002**, *626*, 377–394. [CrossRef]
21. Luminet, J.P. Image of a spherical black hole with thin accretion disk. *Astron. Astrophys.* **1979**, *75*, 228–235.
22. Bhattacharyya, S.; Misra, R.; Thampan, A.V. General Relativistic Spectra of Accretion Disks around Rotating Neutron Stars. *Astrophys. J.* **2001**, *550*, 841–845. [CrossRef]